High-resolution Simulation of Flow and Dispersion of Volcanic SO_2 over the Miyake Island

Naoko Seino, Hidetaka Sasaki, Junji Sato and Masaru Chiba

Meteorological Research Institute, 1-1Nagamine, Tsukuba, Ibaraki 305-0052, Japan
(nseino@mri-jma.go.jp)

Abstract: After severe eruptions of the volcano at Miyake Island in August 2000, a large amount of volcanic gas has been released into the atmosphere. To simulate flows and dispersion of SO_2 gas over the Miyake Island, a set of numerical models was developed. The multi-nesting method was adopted to reflect realistic meteorological field and to sufficiently resolve the flow over the island with a diameter of 8km. The outermost model was the Regional Spectral Model (RSM) of the Japan Meteorological Agency (JMA) with a horizontal grid size of 10km. Finer atmospheric structure was simulated with the nonhydrostatic model jointly developed by the Meteorological Research Institute and the Numerical Prediction Division of JMA (MRI/NPD-NHM) with grid intervals of 2km, 400m and 100m. Lagrangian particle model was applied to the dispersion model, which is driven by the meteorological field of the 100m-grid MRI/NPD-NHM. The random walk procedure was used to represent the turbulent diffusion. The model was verified in four cases. Simulated SO_2 concentrations agreed well with observed concentrations at a monitoring station including temporal variation. Under a large synoptic change, however, accurate prediction became difficult. To further investigate the characteristics of the flow and the distribution of SO_2, numerical experiments have been done. Steady inflows, classified according to surface wind speed and direction, were assumed. Simulated SO_2 distribution on the ground apparently depends on the surface wind. Under relatively weak inflow, there is a large diurnal change in the SO_2 distribution, affected by the thermally induced flow. The SO_2 gas is widely spread downstream in the nighttime but hardly reaches the coastal area in the daytime. On the other hand, little diurnal variation could be seen under the stronger inflow. Ground temperature, as well as the static stability of the inflow, also influences downstream wind, turbulent diffusivity and the SO_2 distribution.

Keywords: Nonhydrostatic model; Multi-nesting; Dispersion model; Volcanic SO_2

1. INTRODUCTION

After a series of volcanism from July 2000, the Mt. Oyama volcano of the Miyake Island made severe eruptions in August 2000 and a large amount of volcanic ash and gaseous materials began to discharge into the atmosphere. The refuge advice for the 3,800 residents of the island was repeated. Finally, the Miyake local government decided to withdraw all the remained residents from the island. From 16 September 2000, the Miyake Island had become vacant.

Emission of the volcanic sulphur dioxide (SO_2) continued after the eruption ceased. The estimated emission rate of SO_2 reached several tens of thousands ton/day in the autumn of 2000. The Miyake Island is located to the 180km south of Tokyo, Japan. Sometimes, advected SO_2 extended to the Tokyo Metropolitan area or neighbouring prefectures and affected atmospheric environment in these regions. Two or three tens of thousands ton/day of SO_2 gas kept emitting still in 2001. High concentration of the SO_2 gas over the island prevents the residents from returning to the Island. However, for the recovery from the damage of basic facilities, several operations of restoration has been started on the Miyake Island.

For the safety operation on the Miyake Island, knowledge of the distribution and concentration of SO_2 gas was urgently required. Since observational data was limited, the numerical modeling is useful for investigating fundamental properties of the volcanic SO_2 gas dispersing over the Miyake Island. A set of the numerical models was proposed (Sasaki et al., 2002) and simulations were conducted with those models.

The main purpose of the present paper is to examine dependencies of the SO_2 distribution and concentration on the land surface upon the atmospheric conditions. In the next section, an outline of the model is described. Results and discussion are presented in Section 3. Concluding remarks are given in Section 4.

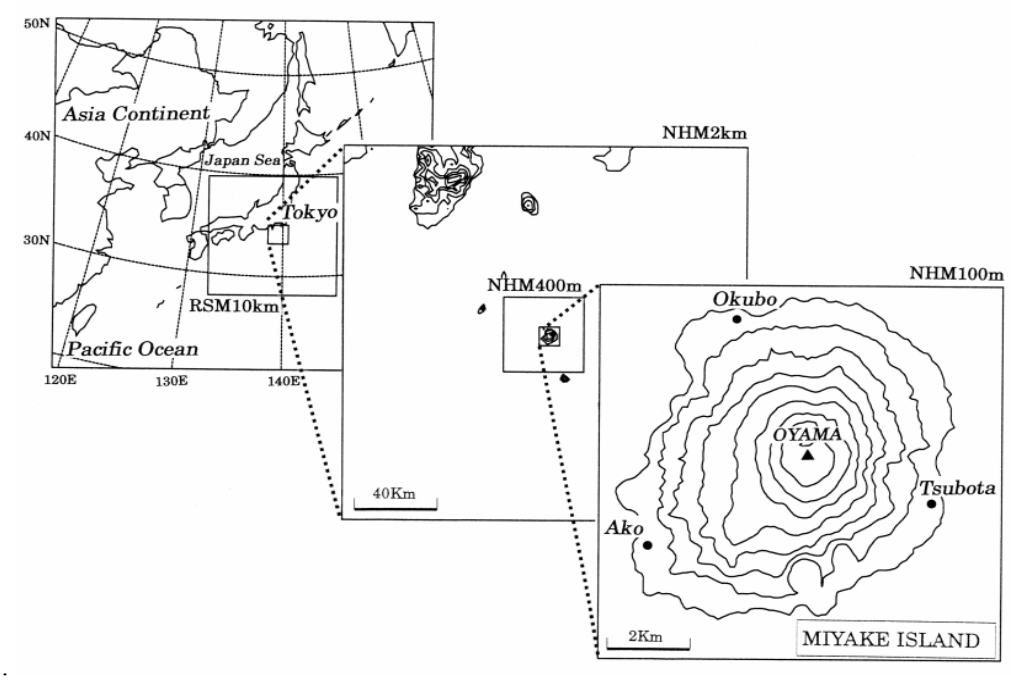

Figure 1. Multi-nesting model domains. Topographic contours (intervals of 100 m) and locations of three monitoring stations on the Miyake Island are shown in the innermost 100m-NHM domain.

2. MODEL

The present modeling system consists of two parts, namely, atmospheric prediction part and dispersion modeling part dealing with SO_2 transport. The former predicts the meteorological variables that drive the latter. The outermost model for the atmospheric prediction is the Regional Spectral Model (RSM) with an equivalent horizontal grid size of 10km. RSM was developed at Japan Meteorological Agency (JMA) and has been used operationally for the weather forecast in the east Asian region (Numerical Prediction Division / JMA, 1997). Using the Global objective analysis data of JMA (GANAL) as initial and boundary conditions for RSM, synoptic conditions can be reflected in the present simulation.

The grid interval of the RSM is, however, too coarse to resolve the flow over the Miyake Island. To simulate finer atmospheric structure under the realistic condition, multi-nesting technique is adopted (Sasaki et al., 1995). The nonhydrostatic model jointly developed by the Meteorological Research Institute and the Numerical Prediction Division of JMA (MRI/NPD-NHM) is utilized as inner models with grid intervals of 2km, 400m and 100m (Saito et al., 2001). The model domain of each nested model is shown in Fig. 1, where topography of the Miyake Island is also drawn.

The Lagrangian particle method is applied to the dispersion model, which is driven by the meteorological field of the 100m-grid MRI/NPD-NHM (100m-NHM). Fundamental scheme of the dispersion model is similar to Sato et al. (1999a, 1999b). Three-dimensional movement of a tracer particle is calculated according to the advection and turbulent diffusion. The random walk procedure is used to represent turbulent diffusion process. The vertical diffusion coefficient is given from the 100m-NHM. The horizontal diffusion coefficient is assumed to be a constant. The dry deposition process is implemented. The wet deposition is, however, excluded in the present simulation, because little condensation and precipitation are expected in the selected cases.

The emission source is set within the crater at the Mt. Oyama. A thousand particles a time step (one second in the present study) are put in a volume of column. The tracer particle corresponds to a fixed weight of the SO_2 gas. Although evaluated amounts of the discharged SO_2 fluctuated day by day, we assume steady release of the SO_2 gas and a constant emission rate of 30 kiloton/day, similar to the average of observations. We also assume that effective radius of the emission R_e is related to the diffusivity at the source area, because the volcanic gas is considered to be suffered the mixing due to the turbulent motion just after the release from the crater. The effective radius of emission is thus given as

$$R_e = \left(1 + \frac{\overline{K}}{3}\right) R_0 \qquad (1)$$

where, K is the vertical diffusion coefficient in the surface layer, overbar signifies horizontal average over the emission area, and R_0 represents the horizontal scale of the release. The tracer particles are initially emitted within R_e. Their number density follows the Gaussian distribution with a horizontal standard deviation $R_e/2$. Vertical deviation of the initial concentration is ignored.

Since discharged volcanic gas has the buoyancy because of the higher temperature than the ambient air, an initial vertical velocity should be added to the particle. The initial rising velocity w_s has also the Gaussian profile around the center of emission.

$$w_s(r) = \frac{w_0}{1-e^{-2}}\left[\exp\left(-2\frac{r^2}{{R_0}^2}\right) - e^{-2}\right] \quad r \le R_0$$
$$= \quad 0 \qquad\qquad R_0 < r \le R_e \quad (2)$$

Here, w_0 represents initial vertical velocity at the center of emission. This means that particles at $R_0 < r\ (<R_e)$ lose their rising velocity as a results of mixing with the ambient air. The vertical velocity of the SO_2 gradually decreased due to the succeeding entrainment. Therefore, temporal variation of the vertical velocity is given as

$$w(t) = \frac{w_s}{1 + w_s\, c_{ent}\, t}. \qquad (3)$$

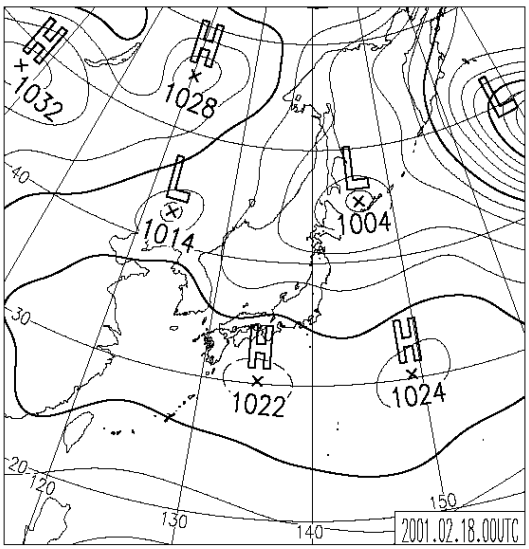

Figure 2. Surface weather chart for 0900 Japan Standard Time (JST) February 2001.

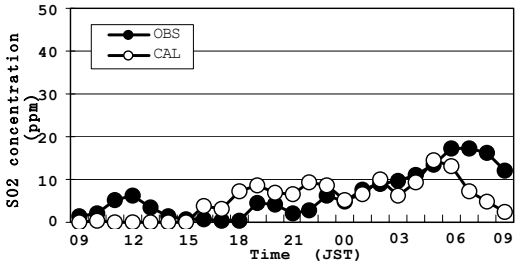

Figure 3. Time series of simulated (open circles) and measured (solid circles) SO_2 concentrations at the Tsubota station from 0900 JST 18 to 0900 JST 19 February 2001.

Here, c_{ent} is a factor of entrainment. The formulation of the rising motion is based on the theory of thermally developed plume (Houze, 1993). The parameters R_0, w_0 and c_{ent} are set to 200 m, 3 m s^{-1} and 0.001 m^{-1} respectively, according to the observation.

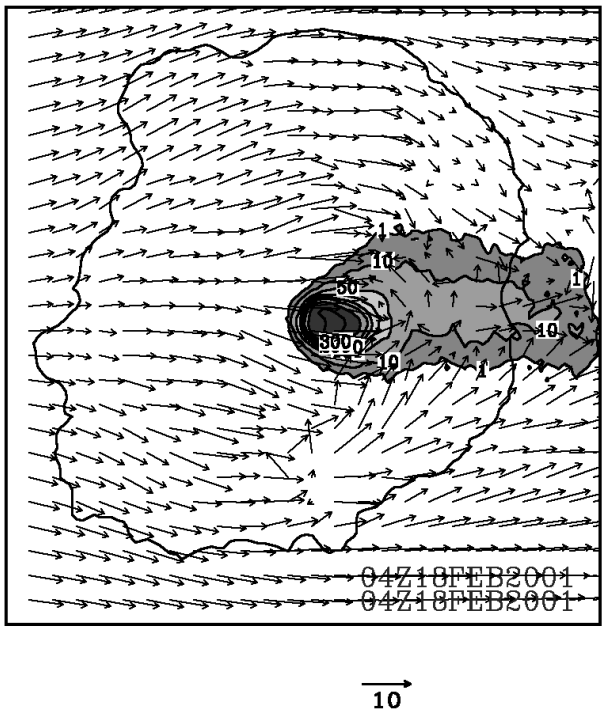

← **Figure 4.** Simulated surface wind vector and SO_2 concentration (shades and contours labeled in ppmv) for 1300JST 18 February 2001.

3. RESULTS AND DISCUSSION

3.1 Comparison with observation

Four cases are selected for the calculation of the SO_2 dispersion. During each selected period, relatively high concentration of SO_2 up to 20

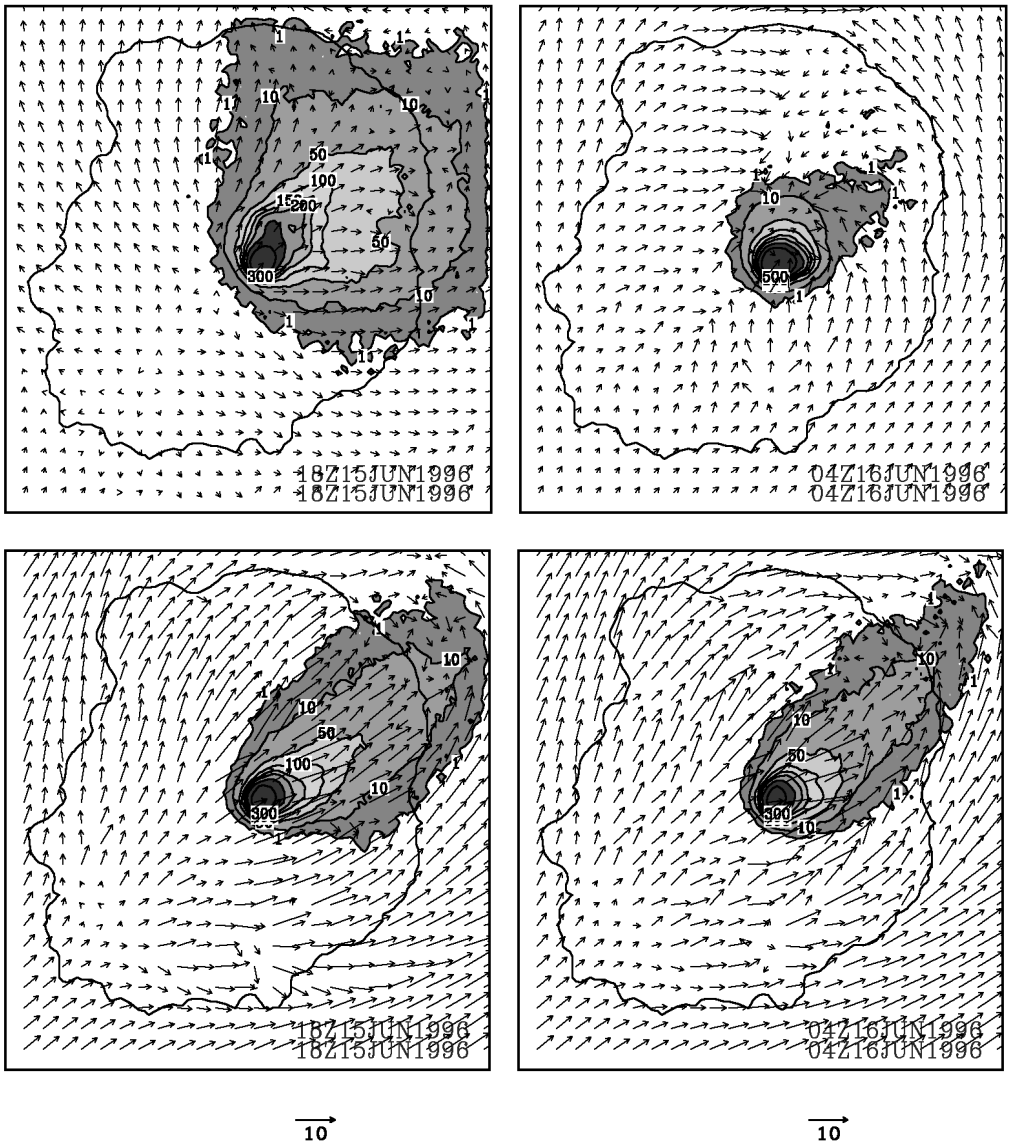

Figure 5. Same as Fig. 4, but for 0300JST of (a) SW02, (b) SW08 and 1300JST of (c) SW02 and (d) SW08.

ppmv was detected at the Tsubota monitoring station (see Fig. 1 for site location). In the present paper, 24-hour simulation results for the 18-19 February 2001 case are shown. In this case, the Miyake Island was located on the northern fringe of the high pressure belt (Fig. 2). Associated westerly winds were observed almost steadily during the period at the station Ako. Such a wind field was well represented in the model.

The simulated time series of the SO_2 concentration agrees well with the measurement, except for the daytime of 18 February (Fig. 3). Figure 4 shows simulated surface SO_2 distributions over the Miyake Island at 1300 JST 18 February.

Temporal variations of the SO_2 concentration at Tsubota were also simulated well in other cases. Under a large synoptic change in the wind field, however, accurate prediction of the concentration became difficult.

3.2 Mean field over the Miyake Island

The simulated results in the four various conditions indicate that the SO_2 gas distribution over the island largely depends on the atmospheric conditions. To examine the characteristics of the SO_2 distribution under various atmospheric structures, further numerical experiments have been done.

First, mean wind and temperature fields over the Miyake Island were evaluated from the Global objective analysis data, GANAL. GANAL is prepared for the operational global forecast of JMA and composed of grid point data at a horizontal interval of 1.25 degrees at the sea or

ground level and upper standard levels. Five years' data in May and June at a vertical column on the grid point nearest the Miyake Island was selected twice a day. Each of data was classified according to sea surface wind speed and direction.

Classif **(c)** into eight wind directions and every 1 m s^{-1} wind speed were adopted in the present study. Averaging the data in each category, a representative wind and temperature profile for the surface wind category was obtained. We can see that south-westerly wind is dominant in this season and 8 m s^{-1} south-westerly surface wind appears most frequently at the selected grid point.

Next, the three dimensional atmospheric field over the Miyake Island was simulated. The mean profile obtained from GANAL was used for initial and boundary conditions of the 400m-NHM as a steady, horizontally uniform basic field for a given wind speed and direction at the sea surface. Conducting the 400m-NHM run, we can obtain the flow over the Island under the steady inflow. Nesting 100m-NHM to 400m-NHM, finer **(d)** spheric field over the Miyake Island was simulated. It should be noted that the simulated flow over the island varies with time because the flow is dynamically disturbed by the mountain and the thermally induced circulations can be caused by the variation of the ground surface temperature. For simplicity, sufficiently small vapour content in the atmosphere is assumed and thus wet deposition associated with moist process is ignored.

3.3 Characteristics of the surface SO_2 distribution

Simulated SO_2 concentrations at the ground surface level apparently depend on the wind speed of the inflow. Figure 5 shows surface SO_2

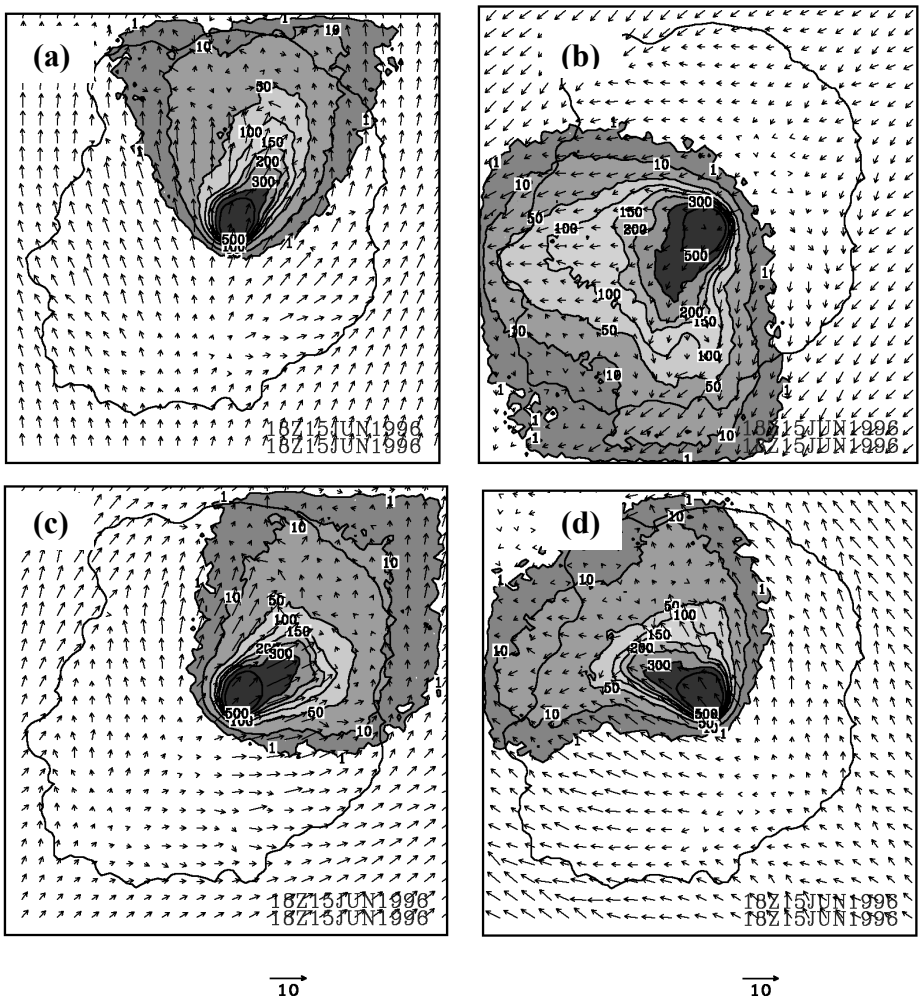

Figure. 6 Same as Fig. 4, but for 0300JST under 4 m s^{-1} wind of (a) S04 (b) NE04 (c) SW04 and (d) SE04.

distributions under the 2 m s^{-1} and 8 m s^{-1} south-westerly inflow (SW02 and SW08). In the SW02 case, high concentration of SO_2 widely spreads to the downstream in the nighttime. In the daytime, on the other hand, the SO_2 hardly reaches the coastal area; because the dispersion of the SO_2 is affected by the upslope component of the surface wind. As the wind speed of the inflow increases, the diurnal variations of the SO_2 concentration and distribution become smaller.

The surface distribution of SO_2 also varies with the direction of inflow (Fig. 6). It can be explained by the difference in the temperature profile of the basic field for each inflow. For example, the north-easterly wind is often associated with the cold inflow in the lower atmosphere. As a result, the mean temperature profile for the north-easterly wind is characterized by relatively high static stability. This leads to the different flow over the island from the south-westerly case, and consequently, the difference in the SO_2 dispersion appears.

Further examination showed that a distinct temporal variation of the SO_2 distribution under the relatively weak wind is related to the change in the turbulent diffusivity in the surface layer that is closely related to the variation of the ground temperature.

4. CONCLUSIONS

A set of numerical models for simulating the dispersion of volcanic SO_2 has been proposed. It included the atmospheric prediction model MRI/NPD-NHM with nonhydrostatic framework and the Lagrangian dispersion model. By means of the multi-nesting technique, realistic atmospheric conditions including large scale tendency can be reflected in the finer models. The innermost model resolves flow over the Miyake Island with a 100m grid interval. The dispersion model is driven by the 100m- grid model output. Both the rising motion of the volcanic gas and mixing process just after the emission from the source are taken into account. The dispersion was successfully carried out in four cases. Concentrations and temporal variations of the SO_2 gas show reasonable agreement between the simulated and observed results at a monitoring station. This demonstrates the reliability of the MRI/NPD-NHM in the fine resolution of 100m grid interval.

Further numerical experiments revealed that basic features of the flow and the dispersion of the SO_2 over the island are dominated by the wind speed and the static stability of the ambient inflow. Ground temperature, as well as the static stability of the inflow, influences downstream wind, turbulent diffusivity and SO_2 distribution. Investigations are still needed to clarify the role of vertical motion in the dispersion process adjacent to the mountain. In addition, the vertical extension of the SO_2 distribution should be examined for the evaluation of the transport in longer range.

5. ACKNOWLEDGEMENTS

The authors thank K. Saito of the Japan Meteorological Agency for giving valuable suggestions. We are grateful to Y. Muraji and S. Hirooka of Energy Sharing Co. Ltd. for their cooperation in the computation. Thanks are extended to T. Matsuo of MRI for his encouragement throughout the work. Numerical computations were conducted using MRI's computer system.

6. REFERENCES

Houze, R. A., Jr., Cloud dynamics, Academic Press Inc., 570pp., 1993.

Numerical Prediction Division / JMA, Outline of the operational numerical weather prediction at the Japan Meteorological Agency, Appendix to Progress Report on Numerical Weather Prediction, 1997.

Saito, K., T. Kato, H. Eito and C. Muroi, Documentation of the Meteorological Research Institute/ Numerical Prediction Division unified Nonhydrostatic Model. Technical Report of the MRI, 42, 133pp., 2001.

Sasaki H., H. Kida, T. Koide and M. Chiba, The performance of a Limited Area Model with a spectral boundary coupling method, *Journal of the Meteorological Society of Japan,* 73(2), 165-181, 1995.

Sasaki H., N. Seino, J. Sato and M. Chiba, Development of dispersion model for volcanic gas over Miyake Island, *Journal of the Meteorological Society of Japan* (submitted), 2002.

Sato J., H. Sasaki and T. Satomura, Transport of sulfur oxides over the east Asian region by the off-line coupled meteorological and transport model, *Papers in Meteorology and Geophysics,* 50(3), 97-111, 1999a.

Sato J., H. Sasaki and K. Adachi, Performance and its evaluation of the MRI long-range transport model for ATMES-II phase of ETEX, *Journal of the Meteorological Society of Japan,* 77(6), 1161-1176, 1999b.